PNAS RESEARCH ARTICLE | IMMUNOLOGY AND INFLAMMATION

HMGB1 released by mesothelial cells drives the development of asbestos-induced mesothelioma

Joelle S. Suarez[a], Flavia Novelli[a], Keisuke Goto[a,b], Michiko Ehara[c], Mika Steele[a], Jin-Hee Kim[a], Alicia A. Zolondick[a,d], Jiaming Xue[a,e], Ronghui Xu[a], Mai Saito[a], Sandra Pastorino[a], Michael Minaai[a], Yasutaka Takanishi[a], Mitsuru Emi[a], Ian Pagano[a], Andrew Wakeham[f], Thorsten Berger[f], Harvey I. Pass[g], Giovanni Gaudino[a], Tak W. Mak[f,h,i,1], Michele Carbone[a,1], and Haining Yang[a,1]

Contributed by Tak W. Mak; received May 17, 2023; accepted August 9, 2023; reviewed by Timothy R. Billiar and Tom K. Hei

Asbestos is the main cause of malignant mesothelioma. Previous studies have linked asbestos-induced mesothelioma to the release of HMGB1 from the nucleus to the cytoplasm, and from the cytoplasm to the extracellular space. In the cytoplasm, HMGB1 induces autophagy impairing asbestos-induced cell death. Extracellularly, HMGB1 stimulates the secretion of *TNFα*. Jointly, these two cytokines kick-start a chronic inflammatory process that over time promotes mesothelioma development. Whether the main source of extracellular HMGB1 were the mesothelial cells, the inflammatory cells, or both was unsolved. This information is critical to identify the targets and design preventive/therapeutic strategies to interfere with asbestos-induced mesothelioma. To address this issue, we developed the conditional mesothelial HMGB1-knockout (*Hmgb1*$^{\Delta pMeso}$) and the conditional myelomonocytic-lineage HMGB1-knockout (*Hmgb1*$^{\Delta Mylc}$) mouse models. We establish here that HMGB1 is mainly produced and released by the mesothelial cells during the early phases of inflammation following asbestos exposure. The release of HMGB1 from mesothelial cells leads to atypical mesothelial hyperplasia, and in some animals, this evolves over the years into mesothelioma. We found that *Hmgb1*$^{\Delta pMeso}$, whose mesothelial cells cannot produce HMGB1, show a greatly reduced inflammatory response to asbestos, and their mesothelial cells express and secrete significantly reduced levels of *TNFα*. Moreover, the tissue microenvironment in areas of asbestos deposits displays an increased fraction of M1-polarized macrophages compared to M2 macrophages. Supporting the biological significance of these findings, *Hmgb1*$^{\Delta pMeso}$ mice showed a delayed and reduced incidence of mesothelioma and an increased mesothelioma-specific survival. Altogether, our study provides a biological explanation for HMGB1 as a driver of asbestos-induced mesothelioma.

HMGB1 | macrophages | mesothelioma | asbestos | microenvironment

Significance

Millions of people have been and continue to be exposed to asbestos worldwide. Some of them have developed mesothelioma, a malignancy resistant to current therapies. Our findings elucidated the mechanisms responsible for asbestos-induced inflammation and carcinogenesis, as well as the cell types involved. Our results revealed the causative link between the process involving HMGB1 release from mesothelial cells, *TNFα* secretion, macrophage accumulation, atypical mesothelial hyperplasia, and mesothelioma onset. Our data point to the HMGB1 secreted by mesothelial cells as the key target to design therapies aimed at interfering with the early steps of mesothelioma growth.

Diffuse malignant mesothelioma (abbreviated as "mesothelioma") is an extremely aggressive cancer that causes about 3,200 deaths/y in the United States and many more worldwide. Up to 5 to 10% of asbestos workers develop mesothelioma after a latency of 30 to 50 y. Most mesotheliomas are caused by exposure to asbestos. "Asbestos" specifically identifies six among ~400 mineral fibers present in nature that have been used commercially, exposing millions of people to its carcinogenic properties (1–5). The use of asbestos has been banned or severely restricted in the "Western" world since the 1980s; however, the overall use of asbestos is increasing in developing countries (1, 2). One of the main commercial benefits of asbestos is its durability; however, this renders the asbestos placed in buildings, roofs, cement pipes, etc., a severe threat for many generations to come, as it has been estimated that in the United States, over 20 million homes contain asbestos (1). Moreover, asbestos and other carcinogenic fibers naturally present in the environment in Nevada (6), Montana and the Dakotas (7), along the US badlands (1), in some areas of California, Oregon (8), etc., and in many countries (7, 9), can cause mesothelioma in the local populations. Additionally, carriers of germline mutations of *BAP1* and of other tumor suppressor genes may have an increased risk of developing mesothelioma when exposed to asbestos or other carcinogenic mineral fibers (10–12).

When inhaled, asbestos fibers become entrapped in the lungs. Through the lymphatic system, some fibers migrate to the pleura where they may cause pleural mesothelioma, and when exposure is high, the fibers can reach the peritoneum and may cause peritoneal mesothelioma. Deposition of asbestos in these tissues causes inflammation (13). Some types of asbestos fibers (crocidolite and amosite, in particular) persist in tissues for many years; thus, the inflammation becomes chronic and leads to reactive mesothelial hyperplasia, lung fibrosis, pleural plaques, and in some cases over the course of decades to mesothelioma (1, 3–5). Asbestos causes DNA damage by the release of mutagenic

Author contributions: M.C. and H.Y. designed research; J.S.S., F.N., K.G., M. Ehara, M. Steele, J.-H.K., J.X., R.X., and M. Saito performed research; A.W., T.B., H.I.P., and T.W.M. contributed new reagents/analytic tools; J.S.S., F.N., K.G., M. Ehara, J.-H.K., A.A.Z., S.P., M.M., Y.T., M. Emi, I.P., T.W.M., M.C., and H.Y. analyzed data; S.P., M.M., Y.T., and M. Emi discussed the data; and J.S.S., G.G., M.C., and H.Y. wrote the paper.

Reviewers: T.R.B., University of Pittsburgh Medical Center; and T.K.H., Columbia University.

The authors declare no competing interest.

[1]To whom correspondence may be addressed. Email: Tak.Mak@uhnresearch.ca, mcarbone@cc.hawaii.edu, or haining@hawaii.edu.

This article contains supporting information online at https://www.pnas.org/lookup/suppl/doi:10.1073/pnas.2307999120/-/DCSupplemental.

Published September 20, 2023.

oxygen radicals from the inflammatory cells that accumulate around asbestos deposits (14). We have linked asbestos carcinogenesis to the release of high mobility group box 1 (HMGB1), a protein that functions in the nucleus to modulate transcription and protect DNA from environmental DNA damage by contributing to nucleosome assembly (15). HMGB1 is an evolutionarily conserved protein that belongs to the group of nonhistone chromatin-associated proteins (16). We demonstrated that upon asbestos exposure, HMGB1 translocates from the nucleus to the cytoplasm where it induces autophagy through the mTOR-ULK pathway and Beclin 1 phosphorylation, a pro-survival mechanism that helps mesothelial cells to survive asbestos-induced cell death (17). Moreover, HMGB1 is released from the cytoplasm into the extracellular space where HMGB1 acts as a prototypic damage-associated molecular pattern molecule (DAMP).

We found that following asbestos exposure, HMGB1 initiates the inflammatory response largely by promoting *TNFα* secretion from nearby cells which, in turn, activates the NFκB signaling pathway (18–20). Both autophagy and NFκB activation help mesothelial cells survive asbestos exposure (18, 19). Thus, extracellular HMGB1 induces the secretion of *TNFα* and kickstarts the inflammatory process that drives mesothelioma growth over time (18, 21). Mesothelioma emerges from the HMGB1-rich environment surrounding asbestos-exposed cells that actively secrete HMGB1 into the microenvironment promoting mesothelioma growth (21). Gene expression profiling validated HMGB1 as a key regulator of the transcriptional alterations induced by asbestos (22). The relevance of HMGB1 in driving mesothelioma growth is underscored by the observation that pharmacological therapies inhibiting HMGB1 secretion and/or activity, delay and impair mesothelioma growth in mice (21, 23–25). In addition, blocking HMGB1 activity inhibited leukocyte recruitment and peritoneal carcinomatosis in mice (26).

In summary, when asbestos accumulates in the pleura and in the peritoneum, mesothelial cells release HMGB1 attracting granulocytes and macrophages that, in turn, actively secrete HMGB1, driving the inflammatory response that may ensue in mesothelioma. Here, we studied the relative contribution of these cell types to the presence of HMGB1 in the microenvironment that promotes chronic inflammation and drives mesothelioma growth. This information is critical to understand the process of asbestos carcinogenesis and to identify the specific therapeutic targets. We investigated this question in two mouse HMGB1 knockout models, specifically affecting mesothelial cells or the myelomonocytic-lineage.

Results

Tissue-Specific HMGB1 Knockout. To study the independent contributions of mesothelial cells and of the inflammatory cells to HMGB1 secretion that drives mesothelioma development, we used two tissue-specific HMGB1 knockout mouse models: 1) inducible mesothelial conditional HMGB1 knockout ($Hmgb1^{\Delta pMeso}$) that we described in Xue et al. (17) and 2) constitutive myelomonocytic-lineage knockout ($Hmgb1^{\Delta Mylc}$) described in Yanai et al. (27). We induced the knockout status in $Hmgb1^{\Delta pMeso}$ by administering tamoxifen intraperitoneally. In the $Hmgb1^{\Delta pMeso}$ mice, immunohistochemistry (IHC) revealed that about 85 to 90% of mesothelial cells had lost HMGB1 expression, while other cell types, including bone marrow–derived macrophages (BMDMs), uniformly expressed HMGB1 (*SI Appendix*, Fig. S1 *A* and *B*). In the $Hmgb1^{\Delta Mylc}$ mice, IHC staining showed that about 98% of BMDM had lost HMGB1 expression, while the other cell types, including mesothelial cells, maintained HMGB1 expression (*SI Appendix*, Fig. S1*A*). These findings were supported by western blot analysis (*SI Appendix*, Fig. S1*B*) confirming the tissue specificity of the HMGB1 knockouts.

Loss of HMGB1 in Mesothelial Cells Exposed to Asbestos Increased DNA Damage and Decreased *TNFα* Expression. As HMGB1 protects DNA from damage, we investigated whether murine mesothelial cells obtained from $Hmgb1^{\Delta pMeso}$ mice have increased genomic instability when exposed to asbestos. $Hmgb1^{\Delta pMeso}$ mesothelial cells exposed to crocidolite, considered the most carcinogenic type of asbestos (1), displayed significantly more micronuclei ($P < 0.05$) —evidence of genetic damage— compared to wild-type (WT) cells (Fig. 1 *A* and *B*). Moreover, phosphorylation of histone H2A.X (γH2A.X), an early cellular response to DNA double-strand breaks, was substantially increased in $Hmgb1^{\Delta pMeso}$ mouse mesothelial cells compared to WT control cells, exposed to asbestos (Fig. 1*C*).

In parallel studies, we found that $Hmgb1^{\Delta pMeso}$ mesothelial cells exposed to asbestos released significantly higher amounts of proinflammatory histone H3 (28) and nucleosomes ($P < 0.01$) into the media compared to WT control mesothelial cells (Fig. 1 *D* and *E*). This supported our findings that $Hmgb1^{\Delta pMeso}$ mesothelial cells display increased DNA damage following asbestos treatment. However, we observed that asbestos-exposed $Hmgb1^{\Delta pMeso}$ mouse mesothelial cells secreted drastically less *TNFα* into the cell culture medium compared to WT mesothelial cells (Fig. 1*F*), an effect caused by the lack of HMGB1 in these cells (*SI Appendix*, Fig. S1 *A* and *B*). Accordingly, the transcription of mRNA specific for *TNFα* and for its receptor *TNFRI* was significantly reduced ($P \leq 0.001$ and $P < 0.05$, respectively) compared to mesothelial cells from WT mice (Fig. 1*G*).

In summary, these results revealed that $Hmgb1^{\Delta pMeso}$ mesothelial cells lacking HMGB1 are more susceptible to asbestos-induced DNA damage and thus might be more susceptible to malignant transformation. On the other hand, these same cells do not secrete HMGB1 and *TNFα*, the cytokines that drive asbestos-induced inflammation and promote mesothelioma (18, 19). These findings raised an intriguing question: Which of the two effects would prevail? Would these mice be more or less susceptible to asbestos carcinogenesis?

HMGB1 Originating from Mesothelial Cells Triggered the Inflammatory Response Supporting Asbestos-Induced Mesothelioma. To investigate the role of HMGB1 in asbestos-induced carcinogenesis in vivo, we conducted short-term and long-term experiments in $Hmgb1^{\Delta pMeso}$ and $Hmgb1^{\Delta Mylc}$ mice. We administered 0.5 mg/mouse of crocidolite intraperitoneally (i.p.) once a week for 10 wk in $Hmgb1^{\Delta pMeso}$, $Hmgb1^{\Delta Mylc}$, and corresponding WT controls $Wt1^{CreERT2/+}$-$Hmgb1^{+/+}$ (control for $Hmgb1^{\Delta pMeso}$ mice) and $LysM^{Cre/+}$-$Hmgb1^{+/+}$ (control for $Hmgb1^{\Delta Mylc}$ mice) (8 to 12 wk old). The same asbestos injection protocol was used for both the short-term experiment to study inflammation and the tissue response (13 mice per group) and for the long-term experiment to study tumor development (40 mice per group). The number of mice per group was based on power analyses (*Materials and Methods* and *SI Appendix*, Fig. S2).

Short-term experiment. One wk following the completion of the 10-weekly crocidolite i.p. injections, mice were euthanized, and a complete necropsy was conducted. Tissues from the organs of the abdominal cavity and from any organ/tissue showing possible lesions were collected. All mice in each group (see above) had diffuse mesothelial cell hyperplasia and chronic inflammation nearby asbestos deposits in the abdominal organs, with formation

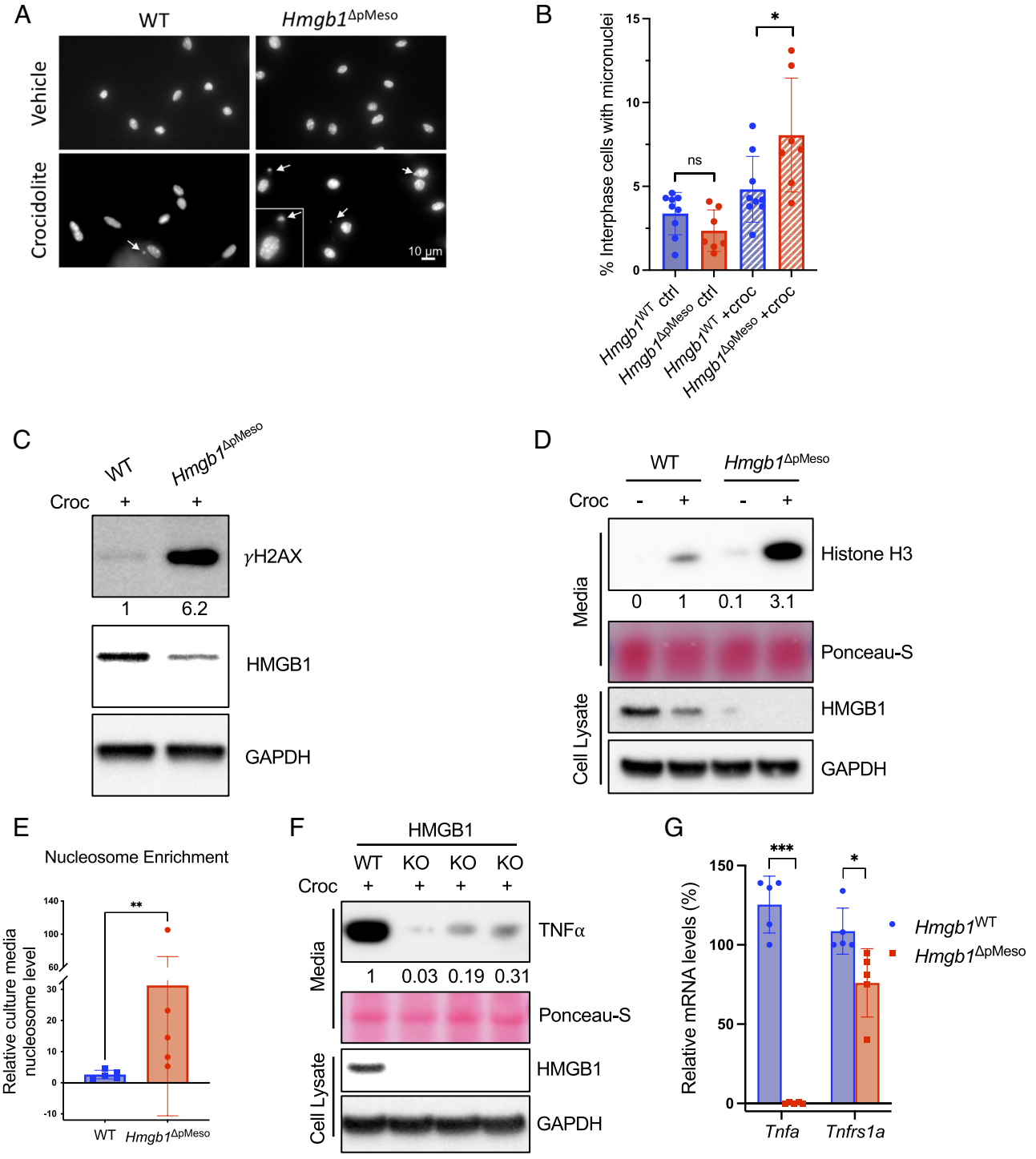

Fig. 1. *Hmgb1*$^{\Delta pMeso}$ mouse mesothelial cells exposed to asbestos show increased DNA damage and nDAMP release and decreased *TNFα* expression. (*A* and *B*) DAPI staining: micronuclei formation upon crocidolite-asbestos exposure. Primary murine mesothelial cells isolated from *Hmgb1*$^{\Delta pMeso}$ mice and WT controls; chromosomal instability was determined as micronuclei frequency at interphase. (*A*) Cells were treated with 5 µg/cm^2 crocidolite for 8 h or untreated (PBS); 48 h later, the number of micronuclei (indicated by white arrows) was measured. (Scale bar, 10 µm.) (*B*) Percentage of interphase cells with micronuclei in ≥100 cells counted per treatment from n = 9 WT and n = 7 *Hmgb1*$^{\Delta pMeso}$ mice in n = 4 independent experiments; data are shown as mean ± SD; *P* values were calculated using a two-tailed unpaired Student's *t* test (*$P < 0.05$) (*C*) Representative immunoblot: DNA damage measured as increased phosphorylation of histone H2A.X (γH2A.X) in murine mesothelial cells exposed to 5 µg/cm^2 crocidolite for 8 h. Decimals: γH2A.X/GAPDH (*D*) Representative immunoblot: histone H3 protein levels in conditioned cell culture media of primary mesothelial cells exposed for 48 h to 5 µg/cm^2 of crocidolite, from *Hmgb1*$^{\Delta pMeso}$ mouse compared to WT littermates. Decimals: Histone H3/Ponceau S (*E*) ELISA to measure nucleosome levels in the same culture media shown in *D*; results are shown as mean ± SD (n = 5). Comparison between *Hmgb1*$^{\Delta pMeso}$ and WT groups was calculated using the Mann–Whitney *U* test for rank comparisons. (**$P < 0.01$) (*F*) Representative immunoblot of *TNFα* protein levels in conditioned cell culture media of primary mesothelial cells exposed for 48 h to 5 µg/cm^2 of crocidolite from *Hmgb1*$^{\Delta pMeso}$ mice compared to WT littermates. Decimals: *TNFα*/Ponceau S (*G*) qRT-PCR: *TNFα* and *TNFR1* mRNA expression levels (*Tnfa* and *Tnfrs1a*) in ex vivo cultured primary murine mesothelial cells from *Hmgb1*$^{\Delta pMeso}$ mice (n = 5) compared to WT controls (n = 5). Data are shown as mean ± SD. *P* values were calculated using a two-tailed unpaired Student's *t* test *($P < 0.05$); **($P < 0.01$); ***($P < 0.001$).

of multiple granulomas and of bowel-to-bowel and bowel-to-organ adhesions. The granulomas in *Hmgb1*$^{\Delta pMeso}$ mice were significantly smaller ($P < 0.01$) compared to those found in WT control mice (Fig. 2 *A* and *B*). IHC studies of biopsies taken from the diaphragm containing granulomas and areas of mesothelial hyperplasia nearby asbestos deposits from *Hmgb1*$^{\Delta pMeso}$ mice showed a significant ($P < 0.05$) increase in CD86$^+$ (M1) macrophages and a significant reduction ($P < 0.001$) in CD206$^+$ (M2) macrophages compared to controls (Fig. 2 *C* and *D*). In areas of mesothelial cell hyperplasia and granulomas, WT mice showed strong *TNFα* IHC staining compared to minimal staining in *Hmgb1*$^{\Delta pMeso}$ mice ($P < 0.001$, Fig. 2 *E* and *F*). In contrast, IHC revealed a strong intensity of *TNFα* staining of the mesothelial cells, granulocytes, and macrophages forming the granulomas surrounding asbestos fibers in myelomonocytic-lineage knockout (*Hmgb1*$^{\Delta Mylc}$) mice, similar to their control WT mice (*SI Appendix*, Fig. S3*A*).

The peritoneal lavage of *Hmgb1*$^{\Delta pMeso}$ mice had significantly ($P < 0.01$) lower amounts of HMGB1 compared to WT mice (Fig. 2*G*). Instead, at this same time point, we observed no significant difference in the concentrations of HMGB1 in the peritoneal lavage of *Hmgb1*$^{\Delta Mylc}$ mice compared to their WT controls (*SI Appendix*, Fig. S3*B*).

Altogether, these findings indicate that mesothelial cells are the primary source of extracellular HMGB1 within the first 10 wk of asbestos exposure and that HMGB1 levels influence the type and intensity of the inflammatory response.

HMGB1 Secretion Modulates the Inflammatory Cell Type Response. As extracellular HMGB1 initiates the inflammatory response following asbestos exposure, we investigated the role of HMGB1 secreted from mesothelial cells versus myelomonocytic-lineage cells in regulating the inflammatory cell type response surrounding asbestos deposits. To quantify total and subset-specific leukocytes, we performed flow cytometry on the cells present in the peritoneal lavage. After the exclusion of cellular aggregates, debris, and dead cells, immune cells were identified using the pan-hematopoietic marker CD45. CD45$^+$ leukocytes represented 95 to 99% of the total cells recovered in each mouse group (Fig. 3*A*). The total number of leukocytes collected from WT, *Hmgb1*$^{\Delta pMeso}$, or *Hmgb1*$^{\Delta Mylc}$ mice was not significantly different (Fig. 3 *A* and *C* and *SI Appendix*, Fig. S4*A*). However, the overall number of Ly6G$^+$ neutrophils in *Hmgb1*$^{\Delta pMeso}$ mice was significantly lower compared to their WT control ($2.4 \pm 0.96 \times 10^5$cells vs. $3.8 \pm 0.66 \times 10^5$, $P = 0.0301$; Fig. 3 *B* and *D*). In contrast, there was no significant difference in the overall number of Ly6G$^+$ neutrophils between *Hmgb1*$^{\Delta Mylc}$ mice and their WT control (*SI Appendix*, Fig. S4*B*). These data suggest that HMGB1 released by mesothelial cells function as a chemoattractant for granulocytes.

As for the macrophages, the overall number of F4/80$^+$ cells (macrophages) was not significantly different in either *Hmgb1*$^{\Delta pMeso}$ or *Hmgb1*$^{\Delta Mylc}$ mice compared to the WT controls (Fig. 3 *B* and *E* and *SI Appendix*, Fig. S4*C*). However, characterization of the macrophage subtypes revealed significant alterations in macrophage polarization in *Hmgb1*$^{\Delta pMeso}$ and *Hmgb1*$^{\Delta Mylc}$ mice exposed to asbestos compared to WT controls. Specifically, we observed a significant increase in the relative percentage of M1-activated macrophages (F4/80$^+$CD86$^+$CD206$^-$), which was paralleled by a corresponding decrease in the percentage of M2 macrophages (F4/80$^+$CD86$^-$CD206$^+$) in both *Hmgb1*$^{\Delta pMeso}$ and *Hmgb1*$^{\Delta Mylc}$ mice compared to WT controls ($P = 0.0024$; Fig. 3 *F* and *G* and *SI Appendix*, Fig. S4 *D* and *E*). No significant changes were observed in other macrophage subtypes in *Hmgb1*$^{\Delta pMeso}$, while a decrease in the macrophage subpopulation CD86$^+$CD206$^+$ was present in the lavage from *Hmgb1*$^{\Delta Mylc}$ mice (*SI Appendix*, Fig. S4 *F* and *G*).

As M1 classically activated macrophages are proinflammatory, we assessed the cytokine and chemokine profiles in the peritoneal lavages of these same mice using a Luminex cytokine/chemokine multiplex kit. Compared to WT controls, the levels of interleukin-3 (IL-3) and of interleukin-10 (IL-10) were significantly lower ($P \leq 0.003$) in the peritoneal lavage from *Hmgb1*$^{\Delta pMeso}$ mice exposed to asbestos (Fig. 4 *A* and *B*). IL-3 is mainly produced by activated T cells and modulates myelomonocytic differentiation (29). IL-10 is mainly produced by M2 macrophages and promotes tumor cell proliferation (30). Since M2 macrophages in *Hmgb1*$^{\Delta pMeso}$ mice were proportionally decreased compared to M1, this finding was expected. The chemokine receptor ligand KC (CXCL1) was instead significantly ($P \leq 0.003$) increased in the peritoneal lavage from *Hmgb1*$^{\Delta pMeso}$ mice compared to WT controls (Fig. 4*C*). CXCL1 is produced by a variety of immune cells and promotes T cell differentiation (31).

Hmgb1$^{\Delta Mylc}$ mice exposed to asbestos displayed significantly lower levels of interleukin-4 (IL-4) and of interleukin-5 (IL-5) compared with WT controls (Fig. 4 *D* and *E*). Both IL-4 and IL-5 modulate T and B lymphocyte functions; both are located on the same Th2 cytokine locus and are usually transcribed together (32, 33). Thus, their reduction implies an alteration in T cell response (32). No significant differences were observed in any other cytokines and chemokines studied in either strain of mice (*SI Appendix*, Fig. S5).

Together, the data of the short-term response to asbestos in *Hmgb1*$^{\Delta pMeso}$ mice and in *Hmgb1*$^{\Delta Mylc}$ mice suggest that 1) the HMGB1 secreted by mesothelial cells drives the initial phase of inflammation caused by asbestos deposition in tissue, and 2) reduced HMGB1 release at the site of asbestos deposits leads to an inflammatory infiltrate rich in M1 proinflammatory macrophages and fewer M2 macrophages, which have anti-inflammatory and tissue remodeling activity.

HMGB1 Knockout in the Mesothelial Lineage Reduces Mesothelioma Development.

Long-term experiment. To investigate whether and how the different expression levels of HMGB1 in mesothelial cells and in myelomonocytic cells influenced asbestos carcinogenesis, we injected 5 mg of crocidolite i.p. (10 injections of 0.5 mg per mouse once a week for 10 wk) to *Hmgb1*$^{\Delta pMeso}$, *Hmgb1*$^{\Delta Mylc}$, and the following control mice: *Hmgb1*$^{+/+}$, *Hmgb1*$^{f/f}$, *Wt1*$^{CreERT2/+}$-*Hmgb1*$^{+/+}$, and *LysM*$^{Cre/+}$-*Hmgb1*$^{+/+}$ (40 mice per group).

Hmgb1$^{\Delta pMeso}$ mice and controls were monitored for 21 mo from the time of the 10th i.p. injection of crocidolite (*SI Appendix*, Fig. S1). During this time, deaths unrelated to asbestos administration occurred in seven *Hmgb1*$^{\Delta pMeso}$ mice, 8 WT mice, and 16 *Wt1*$^{CreERT2/+}$-*Hmgb1*$^{+/+}$ mice (*SI Appendix, Pathology*). The incidence of mesothelioma was significantly lower and mesothelioma developed at a later time in *Hmgb1*$^{\Delta pMeso}$ mice: 21/33 mice developed mesothelioma, 63.6%; $P < 0.0001$; compared with the three control groups: 31 of 32 WT mice developed mesothelioma, 96.9%; 38/40 *Hmgb1*$^{f/f}$ mice developed mesothelioma, 95.0%; and 21/24 *Wt1*$^{CreERT2/+}$ mice developed mesothelioma 87.5%; (Fig. 5*A*). Moreover, *Hmgb1*$^{\Delta pMeso}$ mice had a significantly longer mesothelioma-specific survival (median survival, 450 d; $P = 0.0162$) compared to all three controls (Fig. 5*B* and Table 1). The diagnosis of mesothelioma was unequivocal: It was based on tumor location, histology, and IHC (Fig. 5*C*). Mesotheliomas developed in *Hmgb1*$^{\Delta pMeso}$ mice were smaller and grew largely over the surface rather than infiltrating the abdominal organs, compared to the mesotheliomas that developed in the three control groups. These

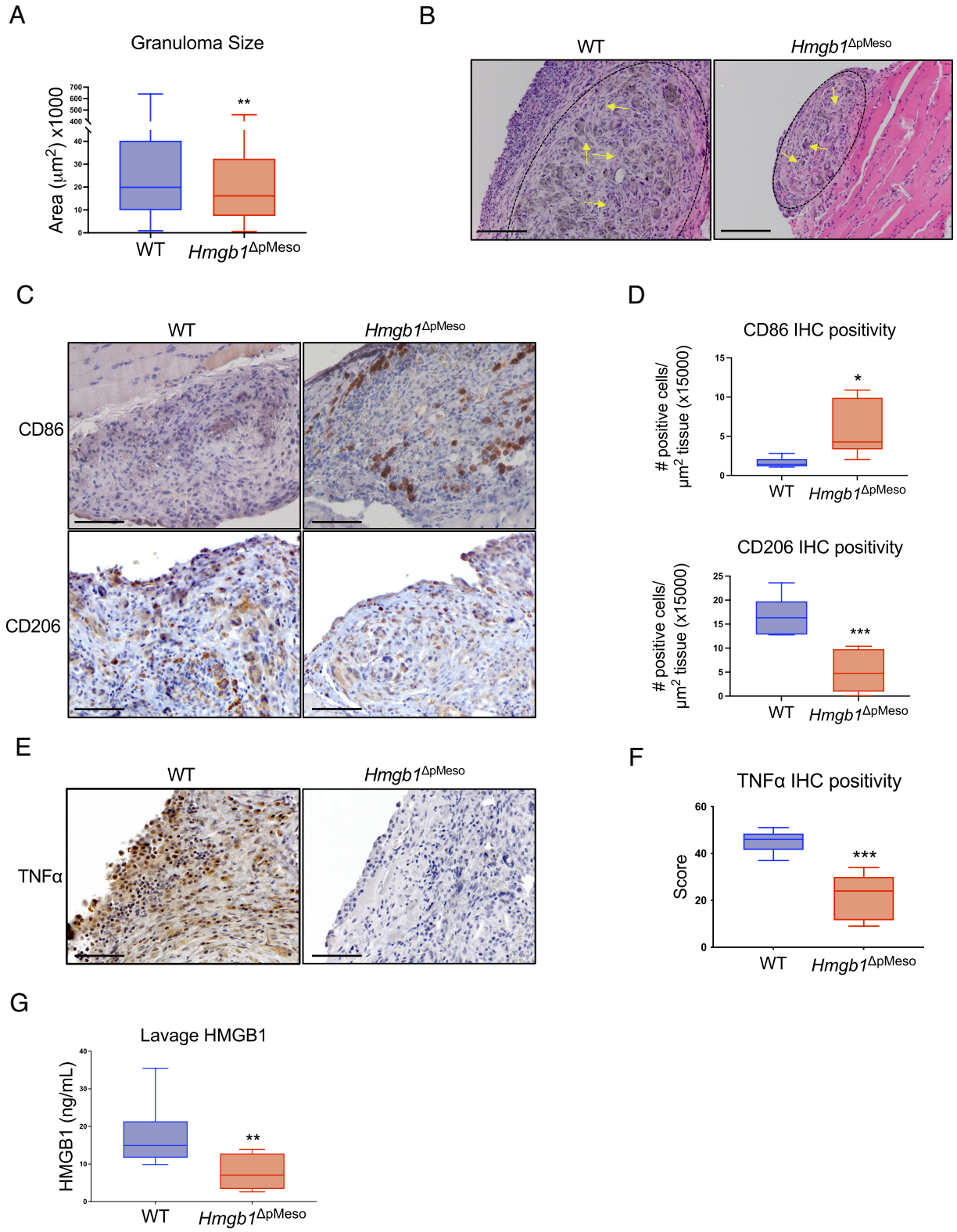

Fig. 2. HMGB1 released from mesothelial cells exposed to asbestos modulates the early inflammatory response. Experiments performed on tissues and lavage from mice injected with 0.5 mg of crocidolite i.p. once/week × 10 wk. Tissues and lavage were collected 1 wk after the 10th injection. (*A*) Decreased granuloma size in peritoneal tissues of *Hmgb1*$^{\Delta pMeso}$ mice (n = 8) compared to WT controls (n = 9). (*B*) Histology. Representative images of granulomas; H&E stain, 200× magnification (Scale bar, 100 μm.) note the reduced size granulomas in *Hmgb1*$^{\Delta pMeso}$ mice compared to controls; arrows indicate asbestos fibers. (*C*) IHC of diaphragm biopsies, 400× magnification (Scale bar, 50 μm.) Note the increased prevalence of CD86^{+} (M1 marker) macrophages and reduced prevalence of CD206^{+} (M2 marker) macrophages in areas of reactive mesothelial hyperplasia of *Hmgb1*$^{\Delta pMeso}$ mice (n = 8), compared to WT controls (n = 9). (*D*) Positive scoring plot of *C*. Box-and-whisker plots display the median, interquartile, and minimum–maximum range. Comparisons between *Hmgb1*$^{\Delta pMeso}$ and WT groups; these were calculated using a two-tailed unpaired Welch's *t* test. (*E*) Representative *TNFα* IHC, diaphragm biopsies, 400× magnification (Scale bar, 50 μm.) Note the decreased/absence *TNFα* stain in the of *Hmgb1*$^{\Delta pMeso}$ mice (n = 8) compared to WT controls (n = 9). (*F*) Positive scoring plot of *E*. (*G*) ELISA for HMGB1. HMGB1 levels measured in the peritoneal lavage of *Hmgb1*$^{\Delta pMeso}$ mice (n = 8) compared to WT controls (n = 9). Box-and-whisker plots display the median, interquartile, and minimum–maximum range. Comparisons between *Hmgb1*$^{\Delta pMeso}$ and WT groups were calculated using a two-tailed unpaired Welch's *t* test. *($P < 0.05$) **($P < 0.01$) ***($P < 0.001$).

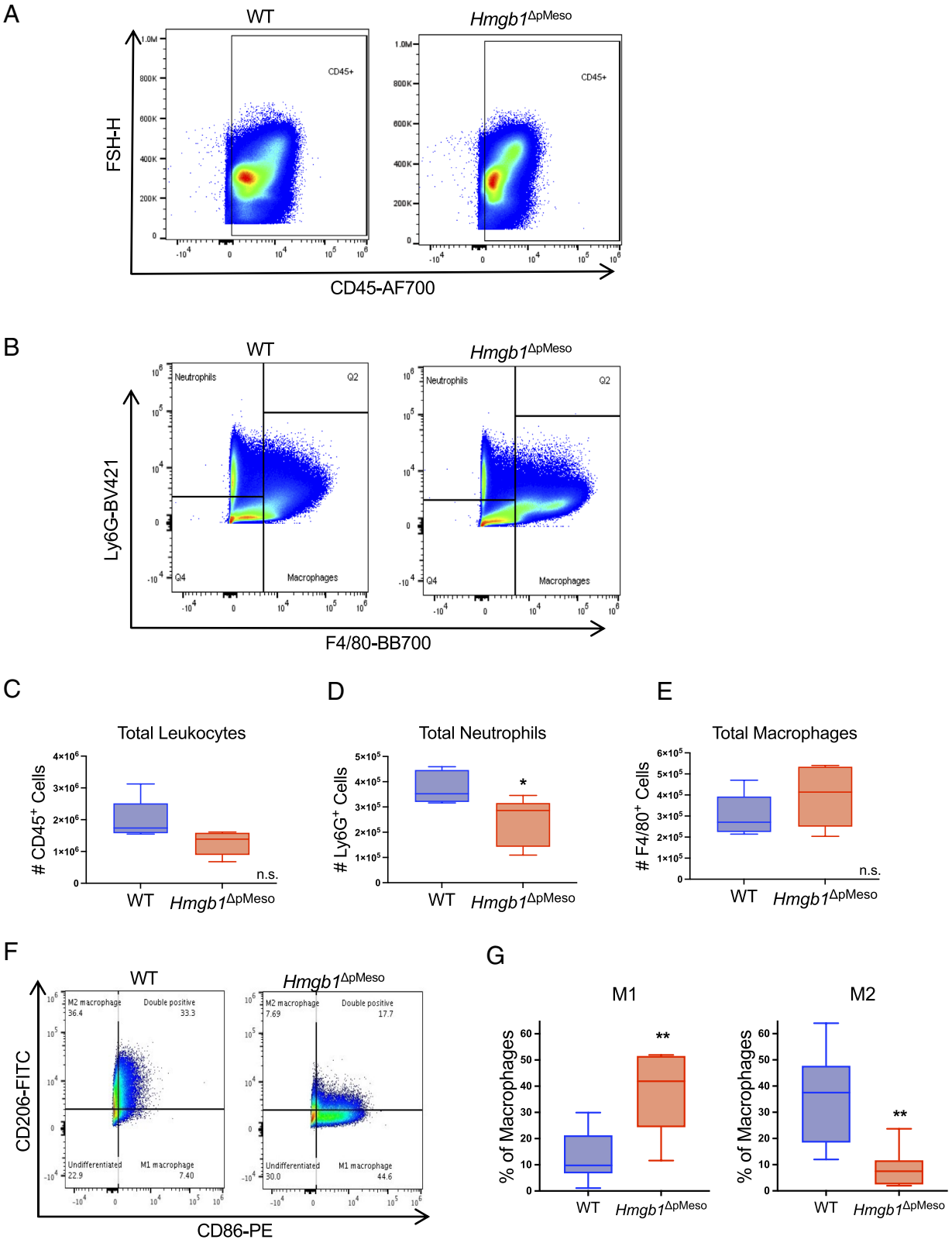

Fig. 3. HMGB1 secretion by mesothelial cells promotes neutrophil recruitment and M2 macrophage polarization. Representative flow cytometry performed on the peritoneal lavage from mice injected i.p. with 0.5 mg of crocidolite i.p. once/week × 10 wk. Peritoneal lavages were collected 1 wk after the 10th injection. The immune cell populations present in the peritoneal lavage were stained for the leukocyte marker CD45, the neutrophil marker Ly6G, and the macrophage marker F4/80, along with macrophage subtype markers CD206 (M2 marker) and CD86 (M1 marker). (*A* and *B*) Dot plots of $CD45^+$ cells and $Ly6G^+$ or $F4/80^+$ cells. (*C*) Total number of $CD45^+$ peritoneal leukocytes collected and subpopulations of (*D*) $Ly6G^+$ neutrophils; (*E*) $F4/80^+$ macrophages from *Hmgb1*$^{\Delta pMeso}$ mice (n = 5) and WT littermates (n = 5). (*F*) Representative flow cytometry dot plots of $CD86^+$ cells and $CD206^+$ cells. (*G*) Increased $CD86^+$ cells and reduced $CD206^+$ cells in *Hmgb1*$^{\Delta pMeso}$ mice (n = 8) compared to WT controls (n = 9). Box-and-whisker plots display the median, interquartile, and minimum–maximum range. Comparisons between *Hmgb1*$^{\Delta pMeso}$ and WT groups were calculated using a two-tailed unpaired Welch's *t* test. *($P < 0.05$) **($P \leq 0.01$).

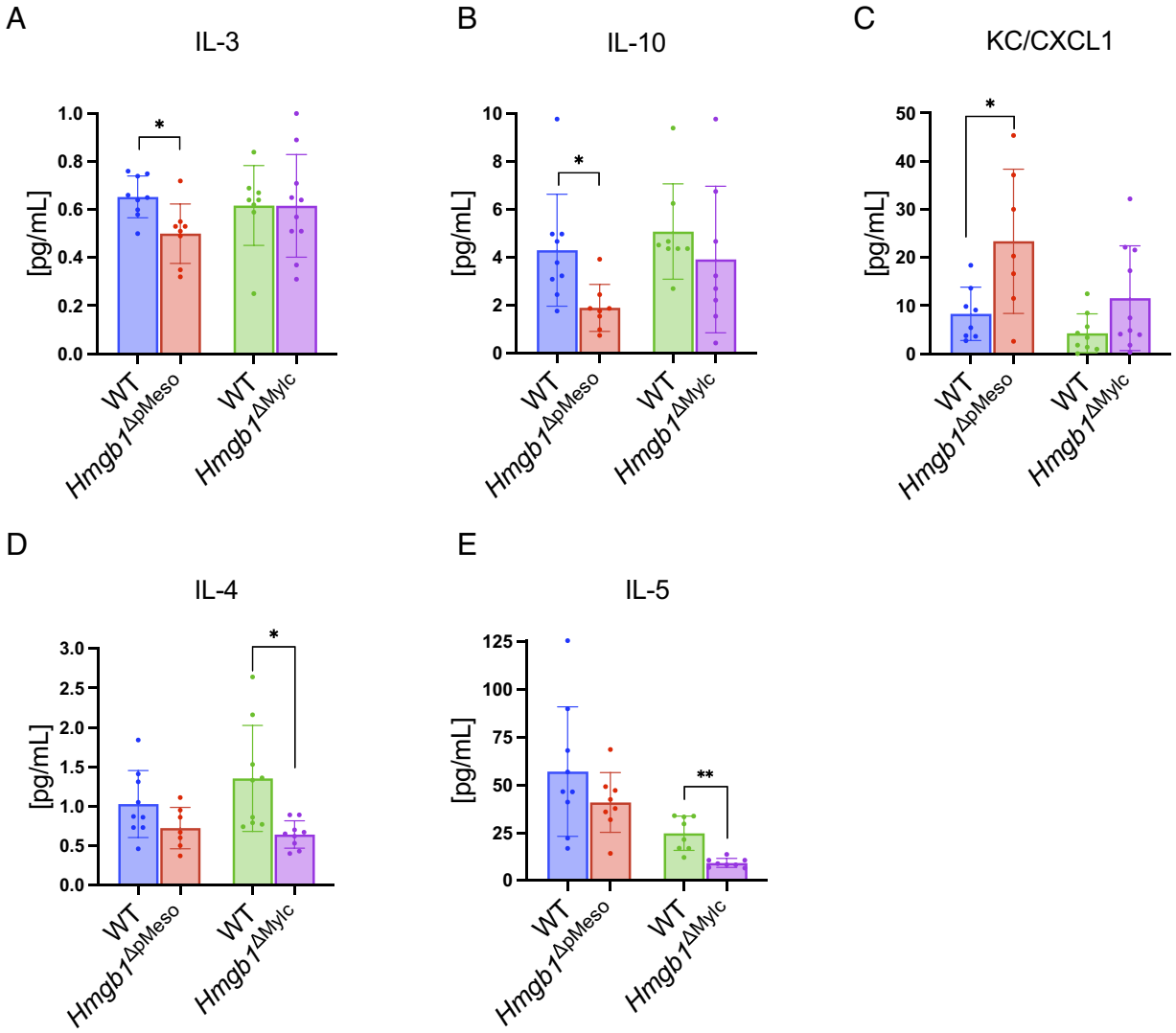

Fig. 4. Mesothelial and myelomonocytic HMGB1 modulates cytokine secretion in mice exposed to crocidolite (i.p. injection). One wk following 10 weekly 0.5 mg crocidolite i.p. injections, the levels of 32 cytokines and chemokines were measured in supernatants recovered from peritoneal lavages using mouse cytokine multiplex kits (EMD Millipore Corporation, Billerica, MA). (*A*–*C*) Altered cytokine levels in the peritoneal lavage of *Hmgb1*$^{\Delta pMeso}$ mice compared to WT controls: (*A*) IL-3, (*B*) IL-10, and (*C*) KC/CXCL1. (*D* and *E*) Altered cytokine levels in the peritoneal lavage of *Hmgb1*$^{\Delta Mylc}$ mice compared to WT controls: (*D*) IL-4 and (*E*) IL-5. Data are shown as mean ± SD; comparisons between *Hmgb1*$^{\Delta pMeso}$ and WT groups were calculated using a two-tailed unpaired Welch's *t* test. *($P \leq 0.003$) **($P < 0.05$).

findings underscored the critical role of HMGB1 released by mesothelial cells in driving mesothelioma growth.

Mesotheliomas are often polyclonal tumors, a result of the carcinogenic field effect of asbestos (34). In the *Hmgb1*$^{\Delta pMeso}$ mesotheliomas, about 20% of WT1-positive mesothelioma cells displayed colocalized nuclear HMGB1 expression, supporting a polyclonal tumor cell population (*SI Appendix*, Fig. S6 *A* and *B*). The number of F4/80+ cells, which are characteristic of macrophages, was significantly reduced in *Hmgb1*$^{\Delta pMeso}$ mesotheliomas (*SI Appendix*, Fig. S6 *A* and *C*). Tumor cells cultured in vitro from the mouse mesotheliomas displayed identical growth rates irrespective of HMGB1 expression (*SI Appendix*, Fig. S7 *A* and *B*). Accordingly, tumor biopsies from these mice showed similar expression of the Ki67 proliferative marker irrespective of HMGB1 expression (*SI Appendix*, Fig. S7 *C* and *D*). These results suggest that HMGB1 modulates the tumor microenvironment rather than the proliferation of mesothelioma cells, and that for those mesothelioma cells not expressing HMGB1, their growth seems not to be impacted by HMGB1 levels (21). We observed significantly more CD3+/CD8+ T cells in the WT mouse mesothelioma biopsies compared to the mesothelioma biopsies from *Hmgb1*$^{\Delta pMeso}$ mice (*SI Appendix*, Fig. S8). Intriguingly, significantly more CD3+/CD8+ cells were present in tissues showing benign mesothelial hyperplasia from *Hmgb1*$^{\Delta pMeso}$ mice 10 wk after asbestos exposure (*SI Appendix*, Fig. S9). These findings suggest that CD3+/CD8+ T cells did not contribute to the reduced tumor growth of mesotheliomas in *Hmgb1*$^{\Delta pMeso}$ mice, although these cells may contribute to the delayed tumor development in these mice.

Hmgb1$^{\Delta Mylc}$ mice could be monitored for only 11 mo because by this time, 36/40 of these mice had died of infection, peritonitis, and intestinal occlusion. Therefore, the surviving 4 mice and their specific control *LysM*$^{Cre/+}$-*Hmgb1*$^{+/+}$ were euthanized, and the experiment was terminated (Table 1). At necropsy, 7/40 of the *Hmgb1*$^{\Delta Mylc}$ mice group had already developed mesothelioma. All *Hmgb1*$^{\Delta Mylc}$ mice had severe chronic peritonitis, multiple adhesions forming among bowel loops, and multiple granulomas around asbestos deposits. Within the control group of this experiment, *LysM*$^{Cre/+}$-*Hmgb1*$^{+/+}$ mice, the survival and cause of death was similar to that observed in the 3 control groups used for the *Hmgb1*$^{\Delta pMeso}$ mice (Table 1).

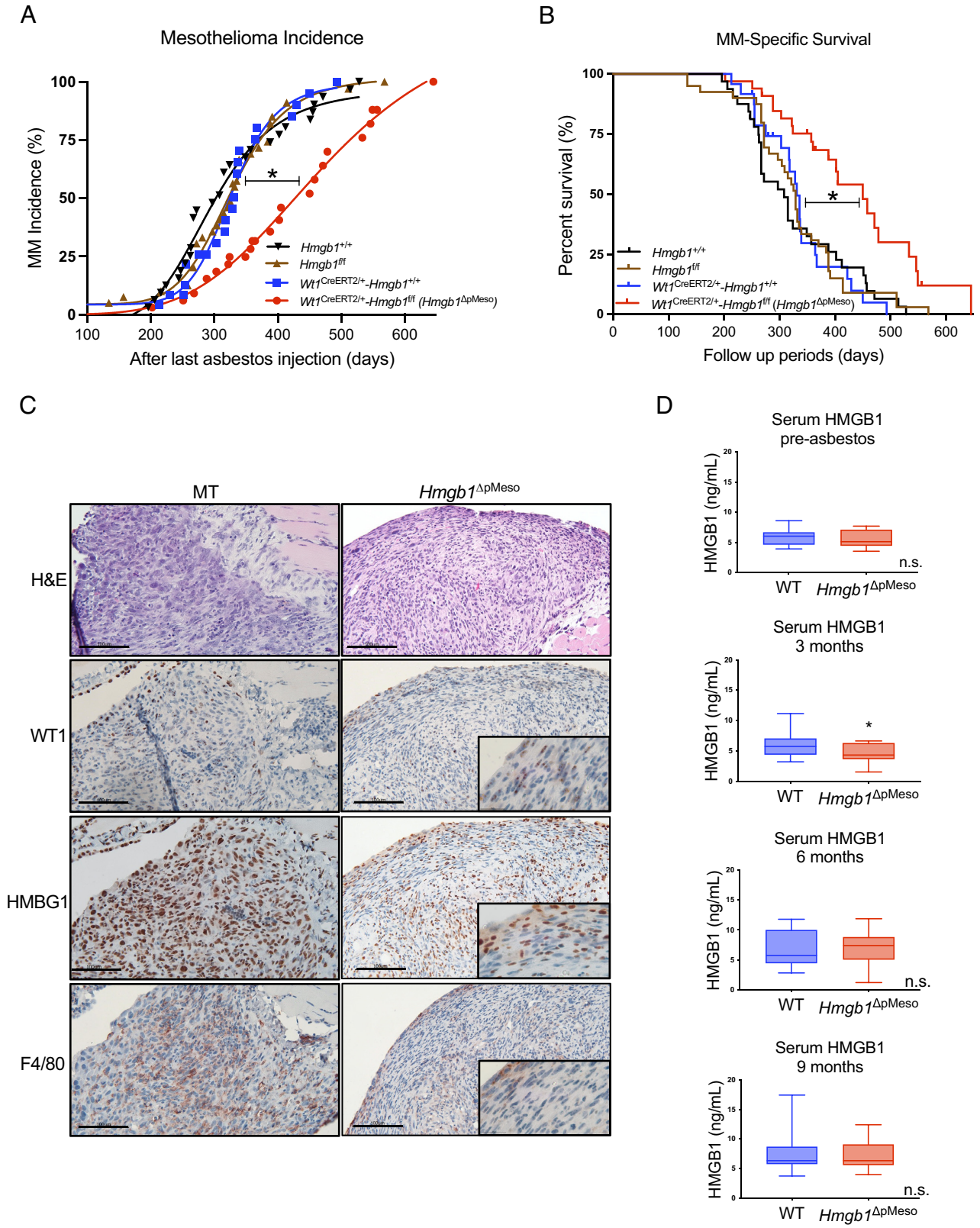

Fig. 5. *Hmgb1*$^{\Delta pMeso}$ mice have an increased latency period between asbestos exposure and mesothelioma development and longer survival. (*A*) Mesothelioma incidence in *Hmgb1*$^{\Delta pMeso}$ mice and in WT controls exposed to asbestos F test. *($P < 0.05$) (*B*) Survival curves of same mice shown in *A*; log-rank (Mantel-Cox) test. *($P < 0.05$). (*C*) Representative mesothelioma biopsies from *Hmgb1*$^{\Delta pMeso}$ mice and WT controls, stained with H/E and the indicated antibodies, 200× magnification (Scale bar, 100 μm.) H/E morphology and positive nuclear WT1 stain identify these tumors as mesotheliomas. Note that HMGB1^{+} and HMGB1^{-} tumor cells in mesotheliomas developed in *Hmgb1*$^{\Delta pMeso}$ mice. Note reduced F4/80 stain (macrophages) in *Hmgb1*$^{\Delta pMeso}$ mice, see text. (*D*) ELISA measuring HMGB1 levels in the serum of *Hmgb1*$^{\Delta pMeso}$ mice (n = 20) compared to WT controls (n = 19) at 3, 6, and 9 mo after asbestos exposure. Box-and-whisker plots display the median, interquartile, and minimum–maximum range. Comparisons between *Hmgb1*$^{\Delta pMeso}$ and WT groups were calculated using a two-tailed unpaired Welch's *t* test. *($P < 0.05$).

Table 1. Mesothelioma Incidence and Survival of HMGB1-cKO Mice

Mouse Genotype	*Hmgb1*$^{+/+}$	*Hmgb1*$^{f/f}$	*Wt1*$^{CreERT2/+}$*Hmgb1*$^{+/+}$	*Wt1*$^{CreERT2/+}$ *Hmgb1*$^{f/f}$ (*Hmgb1*$^{\Delta pMeso}$)	*LysM*$^{Cre/+}$ *Hmgb1*$^{+/+}$	*LysM*$^{Cre/+}$ *Hmgb1*$^{f/f}$ (*Hmgb1*$^{\Delta Mylc}$)
Mesothelioma Incidence	31/32 (97%)	38/40 (95%)	21/24 (88%)	21/33 (64%)	17/33 (52%)	7/22 (32%)
Median Survival	308 d	329 d	331 d	*450 d	N/A	N/A

Hmgb1$^{\Delta pMeso}$ mice had a significantly longer mesothelioma-specific survival (median survival, 450 d; *P = 0.0162) compared to all three controls.

Serum Analyses during the Long-Term Experiment. We collected serum samples before and after completing all asbestos injections from *Hmgb1*$^{\Delta pMeso}$ mice and from its specific control *Wt1*$^{CreERT2/+}$-*Hmgb1*$^{+/+}$ mice, as well as from *Hmgb1*$^{\Delta Mylc}$ mice and its specific control *LysM*$^{Cre/+}$-*Hmgb1*$^{+/+}$ mice. We did not observe any difference in the basal levels of HMGB1 in the serum among either of the HMGB1-cKO mice and their respective control groups prior to asbestos exposure (Fig. 5*D* and *SI Appendix*, Fig. S10*A*). *Hmgb1*$^{\Delta pMeso}$ mice showed a significant ($P < 0.05$) decrease in serum HMGB1 levels compared to WT controls during the first 3 mo following the completion of asbestos injections (Fig. 5*D*). This finding was in line with and supported the reduced amounts of HMGB1 in the peritoneal cavity we detected in the short-term experiment (Fig. 2*G*). However, serum samples taken at 6 and 9 mo did not reveal a sustained significant difference among *Hmgb1*$^{\Delta pMeso}$ and controls (Fig. 5*D*). We attributed this finding to the release of HMGB1 from macrophages that progressively accumulate at sites of chronic inflammation around asbestos deposits in the peritoneum. In *Hmgb1*$^{\Delta pMeso}$ mice, only mesothelial cells cannot express HMGB1; macrophages and other cells contain normal amounts of HMGB1. The *Hmgb1*$^{\Delta Mylc}$ mice, instead, did not show any difference in the concentration of serum HMGB1 during the first 3 mo, but HMGB1 was significantly ($P < 0.05$) reduced compared to controls at 6 mo following asbestos injections (*SI Appendix*, Fig. S10 *B* and *C*). The 9-mo time point in these mice was not collected as too few mice were alive (see above).

Discussion

Our experiments revealed that the HMGB1 released by mesothelial cells in the microenvironment is one of the key modulators of the inflammatory response that leads to the development of asbestos-induced mesothelioma. We found that the size of granulomas and atypical mesothelial hyperplasia that form around asbestos deposit in tissue were significantly reduced in *Hmgb1*$^{\Delta pMeso}$ mice compared to controls. Following asbestos exposure, although *Hmgb1*$^{\Delta pMeso}$ mesothelial cells accumulated more DNA damage and released significantly higher amounts of proinflammatory histone H3 and nucleosomes compared to WT control cells, the inflammatory response to asbestos deposits in the tissues was much less pronounced compared to controls. *TNFα* secretion plays a key role in asbestos-induced inflammation and pathogenesis (19). Accordingly, *TNFα*RKO mice did not develop inflammation and lung fibrosis upon inhalation of asbestos (35). In these *Hmgb1*$^{\Delta pMeso}$ mice, *TNFα* was almost undetectable around asbestos deposits and in the granulomas. Instead, HMGB1 and *TNFα* were strongly expressed by the cells forming the granulomas in all three groups of HMGB1 WT control mice and in the *Hmgb1*$^{\Delta Mylc}$ mice. The significance of these early findings—11 wk post asbestos injection—is supported by the observation that the incidence of mesothelioma was significantly lower in *Hmgb1*$^{\Delta pMeso}$ mice compared to three separate mouse control groups. Furthermore, *Hmgb1*$^{\Delta pMeso}$ mice had a significantly longer mesothelioma-specific survival compared to three control groups. Thus, HMGB1 plays a central role in asbestos-induced mesothelioma (Fig. 6).

It has been reported that the regulatory activities of extracellular HMGB1 are influenced by thiol modifications (36–38). According to these studies, necrotic cells release mainly the all-thiol (reduced form) HMGB1, which can bind the chemokine CXC12 and signal through CXCR4 to induce chemotaxis. Apoptotic cells, on the other hand, release HMGB1 that is partially or completely oxidized at the cysteine residues. Completely oxidized HMGB1 is reportedly unable to stimulate cytokines or induce chemotaxis. Activated macrophages, instead, secrete HMGB1 with C23-C45 disulfide bond and C106 thiol form, which can induce cytokine secretion. Therefore, different HMGB1 redox subtypes may have different activities. Furthermore, these HMGB1 isoforms can be modified by the oxidation status in the microenvironment (37, 38). Asbestos fibers induce ROS that may modify the HMGB1 redox status (14). Therefore, it is difficult to predict the thiol modifications of HMGB1 in a microenvironment characterized by chronic inflammation induced by asbestos fibers. We hope to address this biologically important issue in future studies.

The finding that most tumor nodules in *Hmgb1*$^{\Delta pMeso}$ mice contained both HMGB1-positive and HMGB1-negative mesothelioma cells (about 20% and 80%, respectively) may be related to the field effect of asbestos, which causes mesotheliomas to be polyclonal malignancies (34). This finding also suggests that *Hmgb1*^{WT} mesothelial cells may be more prone to malignant transformation compared to HMGB1-cKO mesothelial cells since in *Hmgb1*$^{\Delta pMeso}$ mice, the HMGB1-expressing mesothelial cells only represent approximately 10% of the total mesothelial cells.

Hmgb1$^{\Delta Mylc}$ mice could only be studied for a limited period of time because these mice, as reported by Dr. Taniguchi (27), were found to be vulnerable to bacterial infection, and therefore, most of them died within 1 y, precluding a complete comparison with the *Hmgb1*$^{\Delta pMeso}$ mice.

Hmgb1$^{\Delta Mylc}$ mice are HMGB1-deficient in both granulocytes and macrophages. We did not expect that granulocytes played a significant role in asbestos pathogenesis since granulocytes only participate in the very early stages of inflammation and are lysed and replaced by macrophages within 1 to 2 d (39, 40). However, we did not know which among macrophages and mesothelial cells were primarily responsible for HMGB1 secretion in response to asbestos deposition in tissue.

We found that during the first months following asbestos exposure, *Hmgb1*$^{\Delta pMeso}$ mice had significantly reduced amounts of HMGB1 in the peritoneal cavity compared to *Hmgb1*$^{\Delta Mylc}$ and control mice. This evidence indicates that mesothelial cells are the primary producer of HMGB1 during the early phases of inflammation caused by asbestos. This interpretation is further supported by the reduced levels of serum HMGB1 observed in *Hmgb1*$^{\Delta pMeso}$ mice at 3 mo time point following asbestos exposure. HMGB1 released by mesothelial cells plays a critical role in inducing inflammation that drives asbestos carcinogenesis. In *Hmgb1*$^{\Delta pMeso}$ mice, only mesothelial cells do not express HMGB1, while macrophages and other immune cells contain normal amounts of HMGB1. The amount of HMGB1 secreted by macrophages in *Hmgb1*$^{\Delta pMeso}$ mice during the first 3 mo post asbestos injection was insufficient to cause a detectable increase in HMGB1 concentrations in the

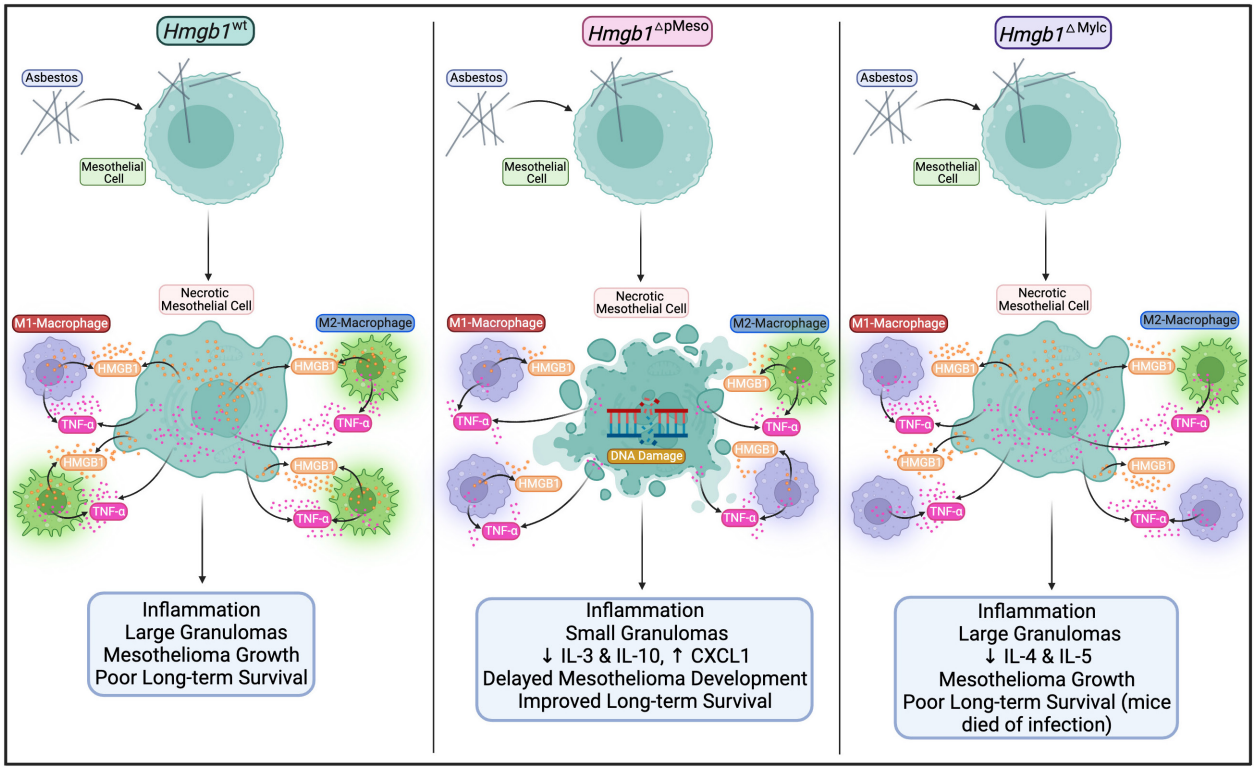

Fig. 6. Schematic representing the major findings in the different HMGB1-cKO mouse models: *Hmgb1*^{WT} (*Left*); *Hmgb1*$^{\Delta pMeso}$ (*Middle*); and *Hmgb1*$^{\Delta Mylc}$ (*Right*). (*Left*) *Hmgb1*^{WT}: In these mice, asbestos causes necrosis of the mesothelial cells that release HMGB1 extracellularly. In the extracellular space, HMGB1 kick-starts the inflammatory process observed upon asbestos deposition in tissues, by promoting *TNFα* secretion and by activating macrophages. Activated macrophages secrete HMGB1 and *TNFα* sustaining inflammation, the formation of large granulomas and promoting mesothelial cell transformation. (*Middle*) *Hmgb1*$^{\Delta pMeso}$: The mesothelial cells of these mice lack HMGB1 and therefore they are more susceptible to asbestos-induced DNA damage and cytotoxicity. These mesothelial cells release low amounts of *TNFα*. In the peritoneal cavity of these mice, we measured low levels of IL-3 and IL-10 and high levels of CXCL1. Macrophages over time accumulated at sites of asbestos deposits secreted HMGB1 and *TNFα* promoting granuloma formation. However, the granulomas were significantly smaller compared to those seen in *Hmgb1*^{WT} mice, mesothelioma growth was delayed, and these mice displayed a significantly improved survival. (*Right*) *Hmgb1*$^{\Delta Mylc}$: Asbestos caused necrotic cell death of *Hmgb1*$^{\Delta Mylc}$ mesothelial cells, HMGB1 release into the extracellular space, and *TNFα* release, as observed in *Hmgb1*^{WT} controls. However, *Hmgb1*$^{\Delta Mylc}$ macrophages do not contain and thus cannot secrete HMGB1. The peritoneal cavity of *Hmgb1*$^{\Delta Mylc}$ mice displayed low levels of cytokines IL-4 and IL-5. These mice had poor overall survival as they were susceptible to bacterial infections. Created with Biorender.com

serum or in the peritoneal fluid and to activate *TNFα* production. At later time points when an increasing number of macrophages accumulate in the peritoneal cavity forming granulomas around asbestos deposits, macrophages became the main producers of HMGB1, and we could no longer detect differences in HMGB1 serum levels among *Hmgb1*$^{\Delta pMeso}$ and controls. Accordingly, the *Hmgb1*$^{\Delta Mylc}$ mice, in which macrophages do not express HMGB1, did not show any difference in the concentration of serum HMGB1 during the first 3 mo, but HMGB1 was significantly ($P < 0.05$) reduced compared to controls at 6 mo after asbestos injections (*SI Appendix*, Fig. S10 *B* and *C*).

We observed a significant increase in the relative percentage of M1-activated macrophages (F4/80$^+$CD86$^+$CD206$^-$) paralleled by a corresponding decrease in the percentage of M2 macrophages (F4/80$^+$CD86$^-$CD206$^+$) in both *Hmgb1*$^{\Delta pMeso}$ and *Hmgb1*$^{\Delta Mylc}$ mice compared to WT controls (Fig. 3 *F* and *G* and *SI Appendix*, Fig. S4 *D* and *E*). Moreover, a decrease in the macrophage subpopulation CD86$^+$CD206$^+$ was present in the lavage from *Hmgb1*$^{\Delta Mylc}$ mice (*SI Appendix*, Fig. S4 *G*). These alterations alone, in the absence of the HMGB1-*TNFα*-driven inflammatory response, were insufficient to induce detectable histological differences among *Hmgb1*$^{\Delta Mylc}$ and controls (*SI Appendix*, Fig. S3*A*), differences that were readily detectable in *Hmgb1*$^{\Delta pMeso}$ mice (Fig. 2*E*).

The development of mesothelioma in *Hmgb1*$^{\Delta pMeso}$ mice was difficult to predict when this work was initiated. On the one hand, these mice lack HMGB1 in the nucleus in most (~90%) mesothelial cells: Since HMGB1 protects DNA from genetic damage (41, 42), these mice should be more susceptible to the genotoxic effects of asbestos. On the other hand, most of the mesothelial cells of *Hmgb1*$^{\Delta pMeso}$ mice do not contain or release HMGB1; thus, these mice should be less susceptible to HMGB1-driven inflammation caused by asbestos exposure. In previous studies, we and others linked extranuclear HMGB1 to *TNFα* release and mesothelioma development (19, 21–23, 43). Here, we found that mesothelial cells from *Hmgb1*$^{\Delta pMeso}$ mice are more susceptible to asbestos-induced genetic damage. However, this increased susceptibility was not sufficient to cause the same high incidence of mesothelioma observed in the 3 control mouse groups which express HMGB1 in all their mesothelial cells and therefore show less genetic damage upon asbestos exposure. Therefore, our results indicate that the HMGB1 released by mesothelial cells into the microenvironment is crucial for mesothelioma development. We found that the HMGB1 released by mesothelial cells in the microenvironment nearby asbestos deposits in tissue promotes the chronic inflammatory response leading to granuloma formation and atypical mesothelial hyperplasia, processes that, over time, may lead to the growth of mesothelioma. Recent studies revealed that also inactivating *BAP1* mutations cause the release of HMGB1 from the nucleus to the cytoplasm and to the extracellular space (23). This finding underscores the central role of HMGB1 in mesothelioma and provides a common mechanistic link among asbestos-induced mesotheliomas and the mesotheliomas that develop in carriers of germline *BAP1* mutations. This common link could be exploited in chemopreventive approaches.

In summary, our findings elucidated the cell types involved in the release of HMGB1 that follows asbestos deposition in tissues and that drive the chronic inflammatory process. The increased DNA damage we observed in mesothelial cells lacking nuclear HMGB1 appeared to play a lesser role in promoting mesothelioma compared to the tumor-promoting role of extracellular HMGB1 and the related inflammatory response because *Hmgb1*$^{\Delta pMeso}$ mice had delayed and reduced mesothelioma formation and improved survival. Our results point to the HMGB1 released by mesothelial cells as the culprit and thus the main target to design therapies to interfere with the pathogenic process caused by asbestos that, over time, may lead to mesothelioma.

Materials and Methods

Animal Models. All animal care and experiments were in accordance with the Association for Assessment and Accreditation of Laboratory Animal Care guidelines (http://www.aaalac.org) and with approval from the University of Hawaii Institutional Animal Care and Use Committee (Protocol # 09-682). *Hmgb1*$^{flox/flox}$ mice, *Wt1*$^{CreERT2/+}$, and *LysM*$^{Cre/+}$ were generated based on the previous publication of Tadatsugu Taniguchi and provided by Tak W. Mak (University of Toronto) for cross-breeding to generate indicated HMGB1 knockout in mesothelial cells (*Hmgb1*$^{\Delta pMeso}$) or in myelomonocyte lineage cells (*Hmgb1*$^{\Delta Mylc}$) (17, 27). All mice were housed under a 12-h light–dark diurnal cycle and provided with a standard rodent chow and water ad libitum throughout all experiments. To study the effects of crocidolite asbestos on mesothelioma tumorigenesis, 8- to 12-wk-old *Hmgb1*$^{\Delta pMeso}$ mice were injected intraperitoneally (i.p.) with 1 mg tamoxifen in corn oil for five consecutive d to induce Cre-recombinase expression. Two wk were given for Cre-mediated HMGB1 recombination to ensue. All mouse groups were subjected to i.p. crocidolite asbestos injection of 0.5 mg once per week for 10 wk.

Asbestos preparation, isolation and culture of murine mesothelial cells, and isolation and culture of murine BMDM, see *SI Appendix*.

Determination of Micronuclei Frequency. Micronuclei from a minimum of 100 interphase cells were quantified in crocidolite-treated cultures, as well as in untreated (PBS only) cultures, four independent experiments (biological replicates: N = 9 WT; N = 7 *Hmgb1*$^{\Delta pMeso}$). See *SI Appendix* for additional details.

Western blot and qRT-PCR analyses were according to standard procedures, see *SI Appendix*.

Cytokines and Chemokines Assay. The levels of 32 cytokines and chemokines were detected in peritoneal lavages and serum samples using murine cytokine/chemokine multiplex kits according to the manufacturer's instructions (EMD Millipore Corporation, cat. no. MCYTMAG-70K-PX32). The filter plate was analyzed using a Luminex® 200™ System, and concentrations of each cytokine were determined using xPONENT® Version 3.1 software. See *SI Appendix* for details.

Flow Cytometry. Cellular fluorescence was measured using an Attune Nxt Flow Cytometer (Invitrogen), and data were analyzed using FlowJo 11 (Becton Dickinson). Antibody concentrations were determined by titration, and BD CompBeads (BD Biosciences) were used to perform compensation. Cutoff gates for positivity were established using the fluorescence-minus-one technique (44). See *SI Appendix*.

ELISA Assays and Growth Curves. HMGB1 (Tecan) levels in serum or peritoneal lavage supernatant were measured using ELISA according to the manufacturer's protocol. Cell proliferation was measured using the CyQuant assay (Thermo Fisher Scientific, C35011). For details, see *SI Appendix*.

Pathology, image analysis, immunofluorescence, and IHC were conducted according to standard procedures. See *SI Appendix*.

Statistical Analysis. Data are presented as mean ± SD. In the long-term exposure to asbestos fibers experiment, survival was measured using the Kaplan–Meier method. Mesothelioma incidence nonlinear-fit and survival curves were compared by the F test and log-rank (Mantel–Cox) test, respectively. Statistical significance was determined using a two-tailed unpaired Welch's *t* test. *P* values < 0.05 were considered statistically significant and marked with asterisks as indicated in the figure legends using GraphPad Prism 9 software.

Data, Materials, and Software Availability. All study data are included in the article and/or *SI Appendix*.

ACKNOWLEDGMENTS. We thank Hugh Luk and Christine Farrar (core facilities of the University of Hawai'i Cancer Center) and Alexandra Gurary (Molecular & Cellular Immunology core of the University of Hawai'i John A. Burns School of Medicine) for their technical assistance and Dr. Tadatsugu Taniguchi (University of Tokyo) for providing Hmgb1-floxed mice. This work utilized a Leica Thunder Live Cell Imaging System that was purchased with funding from a NIH SIG grant 1S10OD028515-01. M.C. and H.Y. report funding from the National Institute of Environmental Health Sciences 1R01ES030948-01 (M.C. and H.Y.), the National Cancer Institute (NCI) 1R01CA237235-01A1 (M.C. and H.Y.), and 1R01CA198138 (M.C.), the US Department of Defense W81XWH-16-1-0440 (H.I.P., T.W.M., M.C., and H.Y.), and from the UH Foundation through donations from the Riviera United-4-a Cure (M.C. and H.Y), the Melohn Family Endowment, the Honeywell International Inc., the Germaine Hope Brennan Foundation, and the Maurice and Joanna Sullivan Family Foundation (M.C.). M.C. has a patent issued for "Methods for Diagnosing a Predisposition to Develop Cancer." M.C. and H.Y. have a patent issued for "Using Anti-HMGB1 Monoclonal Antibody or other HMGB1 Antibodies as a Novel Mesothelioma Therapeutic Strategy" and a patent issued for "HMGB1 As a Biomarker for Asbestos Exposure and Mesothelioma Early Detection". M.C. is a board-certified pathologist who provides consultation for pleural pathology, including medical–legal. H.I.P. and H.Y. report funding from the Early Detection Research Network NCI 5U01CA214195-04. H.I.P. reports funding from Genentech and Belluck & Fox, LLP.

Author affiliations: [a]Thoracic Oncology, University of Hawaii Cancer Center, Honolulu, HI 96813; [b]Department of Urology, Graduate School of Biomedical and Health Sciences, Hiroshima University, Hiroshima 734-8551, Japan; [c]Department of Oral Pathology, Division of Oral Pathogenesis and Disease Control, School of Dentistry, Asahi University, Mizuho Gifu 501-0296, Japan; [d]Department of Molecular Biosciences and Bioengineering, University of Hawaii at Manoa, Honolulu, HI 96822; [e]John A. Burns, School of Medicine, University of Hawai'i, Honolulu, HI 96813; [f]Princess Margaret Cancer Center, University Health Network, Toronto, ON M5G 2M9, Canada; [g]Department of Cardiothoracic Surgery, New York University, New York, NY 10016; [h]Department of Pathology, School of Clinical Medicine, Li Ka Shing Faculty of Medicine, The University of Hong Kong, Hong Kong SAR 999077, China; and [i]Centre for Oncology and Immunology, Hong Kong Science Park, Hong Kong SAR 999077, China

1. M. Carbone *et al.*, Mesothelioma: Scientific clues for prevention, diagnosis, and therapy. *CA Cancer J. Clin.* **69**, 402–429 (2019).
2. M. Carbone, H. Yang, H. I. Pass, E. Taioli, Did the ban on asbestos reduce the incidence of mesothelioma? *J. Thorac. Oncol.* **18**, 694–697 (2023).
3. F. Baumann, J. P. Ambrosi, M. Carbone, Asbestos is not just asbestos: An unrecognised health hazard. *Lancet. Oncol.* **14**, 576–578 (2013).
4. M. Carbone, H. Yang, Mesothelioma: Recent highlights. *Ann. Transl. Med.* **5**, 238 (2017).
5. N. Alpert, M. van Gerwen, E. Taioli, Epidemiology of mesothelioma in the 21(st) century in Europe and the United States, 40 years after restricted/banned asbestos use. *Transl. Lung Cancer Res.* **9**, S28–s38 (2020).
6. F. Baumann *et al.*, The presence of asbestos in the natural environment is likely related to mesothelioma in young individuals and women from southern nevada. *J. Thorac. Oncol.* **10**, 731–737 (2015).
7. M. Carbone *et al.*, Erionite exposure in North Dakota and Turkish villages with mesothelioma. *Proc. Natl. Acad. Sci. U.S.A.* **108**, 13618–13623 (2011).
8. A. Croce *et al.*, Numerous iron-rich particles lie on the surface of erionite fibers from rome (Oregon, USA) and karlik (Cappadocia, Turkey). *Microsc. Microanal.* **21**, 1341–1347 (2015).
9. M. Carbone *et al.*, A mesothelioma epidemic in Cappadocia: Scientific developments and unexpected social outcomes. *Nat. Rev. Cancer* **7**, 147–154 (2007).
10. M. Carbone *et al.*, Medical and surgical care of patients with mesothelioma and their relatives carrying germline BAP1 mutations. *J. Thorac. Oncol.* **17**, 873–889 (2022).
11. A. Bononi *et al.*, Heterozygous germline BLM mutations increase susceptibility to asbestos and mesothelioma. *Proc. Natl. Acad. Sci. U.S.A.* **117**, 33466–33473 (2020).
12. M. Carbone *et al.*, Tumour predisposition and cancer syndromes as models to study gene-environment interactions. *Nat. Rev. Cancer* **20**, 533–549 (2020).
13. G. Liu, P. Cheresh, D. W. Kamp, Molecular basis of asbestos-induced lung disease. *Annu. Rev. Pathol.* **8**, 161–187 (2013).
14. A. Xu, H. Zhou, D. Z. Yu, T. K. Hei, Mechanisms of the genotoxicity of crocidolite asbestos in mammalian cells: Implication from mutation patterns induced by reactive oxygen species. *Environ. Health Perspect.* **110**, 1003–1008 (2002).
15. T. Bonaldi *et al.*, Monocytic cells hyperacetylate chromatin protein HMGB1 to redirect it towards secretion. *EMBO J.* **22**, 5551–5560 (2003).
16. M. E. Bianchi, A. Agresti, HMG proteins: Dynamic players in gene regulation and differentiation. *Curr. Opin. Genet. Dev.* **15**, 496–506 (2005).

17. J. Xue *et al.*, Asbestos induces mesothelial cell transformation via HMGB1-driven autophagy. *Proc. Natl. Acad. Sci. U.S.A.* **117**, 25543–25552 (2020).
18. H. Yang *et al.*, Programmed necrosis induced by asbestos in human mesothelial cells causes high-mobility group box 1 protein release and resultant inflammation. *Proc. Natl. Acad. Sci. U.S.A.* **107**, 12611–12616 (2010).
19. H. Yang *et al.*, TNF-alpha inhibits asbestos-induced cytotoxicity via a NF-kappaB-dependent pathway, a possible mechanism for asbestos-induced oncogenesis. *Proc. Natl. Acad. Sci. U.S.A.* **103**, 10397–10402 (2006).
20. Y. Le *et al.*, Cigarette smoke-induced HMGB1 translocation and release contribute to migration and NF-κB activation through inducing autophagy in lung macrophages. *J. Cell Mol. Med.* **24**, 1319–1331 (2020).
21. S. Jube *et al.*, Cancer cell secretion of the DAMP protein HMGB1 supports progression in malignant mesothelioma. *Cancer Res.* **72**, 3290–3301 (2012).
22. F. Qi *et al.*, Continuous exposure to chrysotile asbestos can cause transformation of human mesothelial cells via HMGB1 and TNF-α signaling. *Am. J. Pathol.* **183**, 1654–1666 (2013).
23. F. Novelli *et al.*, BAP1 forms a trimer with HMGB1 and HDAC1 that modulates gene × environment interaction with asbestos. *Proc. Natl. Acad. Sci. U.S.A.* **118**, e2111946118 (2021).
24. H. Yang *et al.*, Aspirin delays mesothelioma growth by inhibiting HMGB1-mediated tumor progression. *Cell Death Dis.* **6**, e1786 (2015).
25. L. Pellegrini *et al.*, HMGB1 targeting by ethyl pyruvate suppresses malignant phenotype of human mesothelioma. *Oncotarget* **8**, 22649–22661 (2017).
26. L. Cottone *et al.*, Leukocytes recruited by tumor-derived HMGB1 sustain peritoneal carcinomatosis. *Oncoimmunology* **5**, e1122860 (2016).
27. H. Yanai *et al.*, Conditional ablation of HMGB1 in mice reveals its protective function against endotoxemia and bacterial infection. *Proc. Natl. Acad. Sci. U.S.A.* **110**, 20699–20704 (2013).
28. R. Chen, R. Kang, X. G. Fan, D. Tang, Release and activity of histone in diseases. *Cell Death Dis.* **5**, e1370 (2014).
29. M. Dougan, G. Dranoff, S. K. Dougan, GM-CSF, IL-3, and IL-5 family of cytokines: Regulators of inflammation. *Immunity* **50**, 796–811 (2019).
30. Z. F. Wen *et al.*, Tumor cell-released autophagosomes (TRAPs) promote immunosuppression through induction of M2-like macrophages with increased expression of PD-L1. *J. Immunother. Cancer* **6**, 151 (2018).
31. L. Jin, S. Batra, D. N. Douda, N. Palaniyar, S. Jeyaseelan, CXCL1 contributes to host defense in polymicrobial sepsis via modulating T cell and neutrophil functions. *J. Immunol.* **193**, 3549–3558 (2014).
32. G. R. Lee, S. T. Kim, C. G. Spilianakis, P. E. Fields, R. A. Flavell, T helper cell differentiation: Regulation by cis elements and epigenetics. *Immunity* **24**, 369–379 (2006).
33. B. L. Kelly, R. M. Locksley, Coordinate regulation of the IL-4, IL-13, and IL-5 cytokine cluster in Th2 clones revealed by allelic expression patterns. *J. Immunol.* **165**, 2982–2986 (2000).
34. S. Comertpay *et al.*, Evaluation of clonal origin of malignant mesothelioma. *J. Transl. Med.* **12**, 301 (2014).
35. J. Y. Liu, D. M. Brass, G. W. Hoyle, A. R. Brody, TNF-alpha receptor knockout mice are protected from the fibroproliferative effects of inhaled asbestos fibers. *Am. J. Pathol.* **153**, 1839–1847 (1998).
36. M. Magna, D. S. Pisetsky, The role of HMGB1 in the pathogenesis of inflammatory and autoimmune diseases. *Mol. Med.* **20**, 138–146 (2014).
37. M. E. Bianchi *et al.*, High-mobility group box 1 protein orchestrates responses to tissue damage via inflammation, innate and adaptive immunity, and tissue repair. *Immunol. Rev.* **280**, 74–82 (2017).
38. D. Tang, R. Kang, H. J. Zeh, M. T. Lotze, The multifunctional protein HMGB1: 50 years of discovery. *Nat. Rev. Immunol.*, 10.1038/s41577-023-00894-6 (2023).
39. C. I. Schoenberger, G. W. Hunninghake, O. Kawanami, V. J. Ferrans, R. G. Crystal, Role of alveolar macrophages in asbestosis: Modulation of neutrophil migration to the lung after acute asbestos exposure. *Thorax* **37**, 803–809 (1982).
40. D. W. Kamp, M. M. Dunn, J. S. Sbalchiero, A. M. Knap, S. A. Weitzman, Contrasting effects of alveolar macrophages and neutrophils on asbestos-induced pulmonary epithelial cell injury. *Am. J. Physiol.* **266**, L84–91 (1994).
41. R. Kang *et al.*, Intracellular Hmgb1 inhibits inflammatory nucleosome release and limits acute pancreatitis in mice. *Gastroenterology* **146**, 1097–1107 (2014).
42. S. S. Lange, D. L. Mitchell, K. M. Vasquez, High mobility group protein B1 enhances DNA repair and chromatin modification after DNA damage. *Proc. Natl. Acad. Sci. U.S.A.* **105**, 10320–10325 (2008).
43. R. Mezzapelle *et al.*, Human malignant mesothelioma is recapitulated in immunocompetent BALB/c mice injected with murine AB cells. *Sci. Rep.* **6**, 22850 (2016).
44. N. Baumgarth, M. Roederer, A practical approach to multicolor flow cytometry for immunophenotyping. *J. Immunol. Methods* **243**, 77–97 (2000).